Significant acceleration of regional brain aging and atrophy after mild traumatic brain injury

Alexander F. Shida, MS[1], Roy J. Massett, BA[1], Phoebe Imms PhD[1], Ramanand V. Vegesna[1], Anar Amgalan, PhD[1], and Andrei Irimia, PhD[1, 2, 3] * for the Alzheimer's Disease Neuroimaging Initiative**

[1] Ethel Percy Andrus Gerontology Center, Leonard Davis School of Gerontology, University of Southern California, Los Angeles, CA, USA

[2] Corwin D. Denney Research Center, Department of Biomedical Engineering, Viterbi School of Engineering, University of Southern California, Los Angeles, CA, USA

[3] Department of Quantitative & Computational Biology, Dana and David Dornsife College of Arts & Sciences, University of Southern California, Los Angeles, CA, USA

*Corresponding author: irimia@usc.edu

**Data used in preparation of this article were obtained from the Alzheimer's Disease Neuroimaging Initiative (ADNI) database (adni.loni.usc.edu). As such, the investigators within the ADNI contributed to the design and implementation of ADNI and/or provided data but did not participate in analysis or writing of this report. A complete listing of ADNI investigators can be found at:

http://adni.loni.usc.edu/wp-content/uploads/how_to_apply/ADNI_Acknowledgement_List.pdf

Abstract

Brain regions' rates of age-related volumetric change after traumatic brain injury (TBI) are unknown. Here we quantify these rates cross-sectionally in 113 persons with recent mild TBI (mTBI), whom we compare against 3418 healthy controls (HCs). Regional gray matter (GM) volumes were extracted from magnetic resonance images (MRIs). Linear regression yielded regional brain ages and the annualized average rates of regional GM volume loss. These results were compared across groups after accounting for sex and intracranial volume. In HCs, the steepest rates of volume loss were recorded in the nucleus accumbens, amygdala and lateral orbital sulcus. In mTBI, ~80% of GM structures had significantly steeper rates of annual volume loss than in HCs. The largest group differences involved the short gyri of the insula and both the long gyrus and central sulcus of the insula. No significant sex differences were found in the mTBI group, regional brain ages being oldest in prefrontal and temporal structures. Thus, mTBI involves significantly steeper regional GM loss rates than in HCs, reflecting older-than-expected regional brain ages.

Keywords

Brain Aging, Imaging, Human Aging, Gender Differences

Abbreviations

AD	Alzheimer's disease
ADNI	Alzheimer's Disease Neuroimaging Initiative
AG	age gap
BA	biological age
CA	chronological age
F	female(s)
FS	FreeSurfer
HC	healthy control
HCP	Human Connectome Project
M	male(s)
MAE	mean absolute error
MRI	magnetic resonance imaging
mTBI	mild traumatic brain injury
TBI	traumatic brain injury
TRACK-TBI	Transforming Research and Clinical Knowledge in TBI

Introduction

Chronological age (CA) is a prominent risk factor for numerous diseases and pathological conditions of the nervous system. However, because aging rates vary from person to person, from body system to body system, and from brain region to brain region (1), biological age (BA) has come to the forefront of recent research as a clinically relevant biomarker of disease risk and mortality (2). BA has been a useful measure to (I) quantify atypical deviations from typical aging in persons affected by disease, (II) assist the process of mapping similarities in the abnormal aging trajectories of persons with various diseases, and (III) estimate the change in conditional risk for a certain disease given the presence of another, as in the case of Alzheimer's disease (AD) risk change after traumatic brain injury (TBI) (3-5). Illustratively, brain BA is often more useful than CA when assessing the risk of neurodegenerative diseases or when predicting their clinical outcomes (6). Recent years have witnessed high interest and considerable success in leveraging magnetic resonance imaging (MRI) to predict brain BA with ever-higher accuracy via machine learning (ML) (3-5,7). Normative patterns of brain aging identified using these approaches in typically aging adults can help to identify and to quantify the pathological alterations of brain structure and/or function observed in conditions ranging from TBI (8) to Parkinson's disease (PD) and AD (5-7). Aside from estimating brain BA from raw MRIs, studies using such approaches have also relied on descriptive properties of individual brain regions (e.g., cortical volume, surface area, mean thickness, mean curvature) to map neural and cognitive features indicative of essential tremors, epilepsy, AD, and multiple sclerosis (9).

Despite the increasing popularity of BA estimation to study these and other brain diseases, an insufficient amount of effort has been devoted to the use of brain BA estimation when studying the effects of TBI on the aging brain (4,8). Even mild TBI (mTBI) can age the brain through oxidative stress, persistent inflammation, and neuronal apoptosis from both primary and secondary injuries (9). Such processes, documented in animals, can be studied only indirectly in humans. In the latter, however, non-invasive MRI is acquired routinely, having revealed mTBI-related chronic atrophy (10)

particularly in the gray matter (11). MRI-derived brain measures are surrogate measures of aging that reflect brain atrophy and that facilitate the estimation of BA as a measure of aging (12).

ML approaches to brain BA estimation offer considerable advantages (3,7). Despite their utility, the results of most ML approaches for BA estimation can be difficult or impossible to interpret due to the black-box nature of ML. Interpretable ML, a class of techniques still in early stages of development, testing, and validation, may soon provide neuroanatomic insights by revealing the brain features whose alterations mirror the most prominent distinctions between typical and abnormal brain aging patterns (13). However, even when such approaches become common, their validation will greatly benefit from the availability of standard, easily interpretable BA estimation models against which interpretable ML frameworks can be validated.

Currently, both white- and black-box solutions for brain BA estimation typically use T_1-weighted structural MRIs to estimate brain BA (2,4). Here we investigate the effects of mild TBI (mTBI) on brain's structure relative to the aging patterns of healthy controls (HCs). In addition, we consider differences in these effects between sexes, as well as sex-dependent regional differences in brain aging in both HCs and mTBIs (13). The link between participants' regional BAs and their cognitive performance was also examined. We choose a cross-sectional design for a wide range of age coverage and due to greater MRI data availability. Our primary goals are to (I) quantify age-related cortical morphology changes in a sex-independent manner, (II) identify regions that change differently with age across sexes, (III) find regions whose aging is affected by mTBI, and to (IV) identify sex dimorphisms in mTBI-related brain structure changes.

Methods

Participants. This study was approved by the Institutional Review Board at the University of Southern California and was carried out in accordance with the U.S. Code of Federal Regulations (45

C.F.R. 46) and with the Declaration of Helsinki. The T_1- and T_2-weighted MRI volumes of HC participants were obtained from the Alzheimer's Disease Neuroimaging Initiative (ADNI, adni.loni.usc.edu) repository (N = 513, 278 females, age: μ = 75 y, σ = 7 y, range: 56 – 95 years (y)), the Human Connectome Project (HCP) Young Adults (YA, N = 1112, 605 females, age: μ = 29 y, σ = 4 y, range: 22 – 37 y, HCP Aging (HCP-A, N = 508, 294 females, age: μ = 56 y, σ = 12 y, range: 36 – 80 y), and the UK Biobank (N = 1285, 676 females, age: μ = 63 y, σ = 10 y, range: 45 – 83 y). The aggregate HC cohort contained N_{HC} = 3418 participants (1853 females; age: μ = 53 y, σ = 19 y, range: 22 – 95 y).

MRIs for N_{TBI} = 113 participants with mTBI were obtained approximately 24 weeks post injury (44 females, age: μ = 43 y, σ = 17 y, range: 21 – 95 y, chronicity: μ = 168 days, σ = 8 days). These MRIs were acquired from subjects recruited with the assistance of board-certified clinicians and of other healthcare professionals. Participant demographics and statistics are listed in **Table 1**. All mTBI MRI data were from mTBI patients with Glasgow Coma Scale (GCS) scores no lower than 13. The GCS objectively quantifies head injury severity based on responsiveness measured by eye-opening, motor, and verbal responses (scores from 3 to 8, 9 to 12, and above 12 indicate TBIs of severe, moderate and mild severity, respectively) (14). Further details, including injury severity, chronicity, and inclusion/exclusion criteria are available in detail in our prior reports (15). Briefly, inclusion criteria were (I) a ground-level fall involving direct head trauma, (II) a GCS score greater than 12, (III) loss of consciousness no longer than 30 minutes, (IV) post-traumatic amnesia of no more than 24 hours, and (V) no evidence of gross TBI pathology on clinical MRI scans. Exclusion criteria were (I) a clinical history of cognitive impairment, neurological and/or psychiatric disease prior to injury and (II) a clinical history of psychotropic substance abuse. Data on head impact location were not available, and rarely are in TBI studies. Although this variable may affect brain aging patterns and their morphometrics (as evidenced by animal studies with more precise experimental control (16)), our inability to account for this factor explicitly motivated our strategy to average results across hemispheres.

Cognitive assessments. Six cognitive measures were obtained using the Brief Test of Adult Cognition Telephone (BTACT) (17), a phone-based cognitive assessment comprising six standard measures of memory, processing speed, verbal fluency, and reasoning described in detail elsewhere (18). Episodic verbal memory (EVM) was quantified using the Rey Auditory Verbal Learning Test, which quantifies immediate recall (EVMI) and delayed recall (EVMD) of a 15-item word list. Working memory span (WMS) was assessed using the backward digit span task. Inductive reasoning (IR) was assessed using a number sequence completion task. Processing speed (PS) was measured using a timed backward counting task. Verbal fluency (VF) was examined using a timed task in which participants name as many items within a category (i.e., animals, male names, and fruit/furniture) as possible.

Neuroimaging. Data acquired by the HCP Consortium were obtained using a protocol described elsewhere and were obtained from the HCP project data repository (https://www.humanconnectome.org). ADNI data used in the preparation of this article were obtained from the ADNI database (https://adni.loni.usc.edu). Currently led by Principal Investigator Michael W. Weiner, MD, the ADNI was launched in 2003 as a public-private partnership. The ADNI's primary goal has been to test whether collection of serial neuroimaging scans, biological markers, and clinical and neuropsychological assessments can be combined to measure the progression of mild cognitive impairment and early AD. For mTBI participants, T_1-weighted MRIs were obtained using a 3D magnetization-prepared rapid acquisition gradient echo sequence with repetition time (T_R) = 1,950 ms, echo time (T_E) = 2.98 ms, inversion time (T_I) = 900 ms, and voxel size = 1.0 mm × 1.0 mm × 1.0 mm. T_2-weighted MRIs were acquired using T_R = 2,500 ms, T_E = 360 ms, and voxel size = 1.0 mm × 1.0 mm × 1.0 mm. Imaging parameters for the publicly available datasets can be found in their respective publications (19-22).

Preprocessing. MRIs acquired from mTBI participants were processed using the freely available FreeSurfer (FS, https://surfer.nmr.mgh.harvard.edu/) software library version 6.0.0 (23,24). HCs'

MRIs were downloaded directly from their respective studies' repositories, for which they had been processed using different FS versions (ADNI: 6.0.0 or 7.1.1; HCP-A: 6.0.0 or 7.1.1; HCP-YA: 5.3.0; UKBB: 6.0.0). Processing included removal of non-brain tissues, transformation into Talairach space, intensity normalization, segmentation into cortical/subcortical structures, surface processing, topology correction, and computation of structure-level volumetrics and morphometrics for 165 brain structures. The values of four types of features (regional cortical volume, surface area, mean cortical thickness, and mean curvature) were adjusted for intracranial volume (ICV), assembled, and then analyzed using the *connectogram* workflow of Irimia et al (25).

Statistical analysis. Because data on head impact location were unavailable, we averaged the values of each feature across hemispheres prior to further analysis. This strategy serves to identify bilateral, rather than unilateral, effects of TBI. Specifically, averaging structures across hemispheres removes structural alterations that are isolated to one hemisphere, which are more likely to be a result of acute focal injury (26). We used averages over hemispheres in a univariate linear fixed-effect regression model (*fitlme*, MATLAB; MathWorks, Natick, MA) to quantify the relationship between CA and each type of feature (volume, surface area, mean curvature, and mean thickness). The statistical effects of study cohort, sex, and FS version were regressed out. For each cohort (HCs and mTBI participants), each feature's annualized mean rate of change β, its standard error (SE) and confidence interval (CI) were calculated as a function of CA and expressed as percentages of the feature's reference value at age 20. For each feature f_i, this was done by fitting a simple linear regression $f_i = \alpha_i + \beta_i CA + \varepsilon_i$. For each region's regression, we tested the null hypothesis $H_0: \beta = 0$ after computing the related t-statistic and associated p-value using the MATLAB *fitlme* function. The statistical significance of group differences in β (e.g., females (F) versus males (M), HC vs mTBI) was tested using a z-test whose statistic $z = (\beta_{TBI} - \beta_{HC})/\sqrt{SE(\beta_{TBI}) + SE(\beta_{HC})}$ pools variance across groups, as recommended by Clogg et al. in the limit of large N, such that the T distribution converges to a Z distribution (27). To compare β across groups within each region, we also calculated both (A) the ratio β_M/β_F for each diagnostic group (HCs and mTBI participants), and

(B) the ratio β_{TBI}/β_{HC} after having regressed out sex effects. The ratio β_{TBI}/β_{HC} of sex-adjusted regression coefficients conveys the factor whereby mTBI participants' annual rate β_{TBI} of age-related volume decrease exceeds HCs' rate β_{HC}. For example, if β_{TBI}/β_{HC} = 2, then mTBI participants exhibit an annualized rate of volume decrease with age that is twice as fast as the reference rate of HCs. We used the Benjamini-Hochberg procedure to correct all p-values for multiple comparisons (28). The statistical power of each test was also computed.

Brain age calculation. For each brain region, we first used a univariate fixed-effect linear regression $CA = \alpha_i + \beta_i v_i + \varepsilon_i$ to estimate the age gap (AG) of region i in HCs by estimating its CA from each regional volume v_i (29). We then implemented bias correction as detailed elsewhere (30). This correction addresses the bias of linear regression when estimating the values of structural features given the ages of the participant. Briefly, estimating BA involves an inherent bias (31,32) because BA estimates become progressively poorer as CAs differ more and more from their sample mean (31). Let BA_b and BA_c be biased (b) and bias-corrected (c) BA. The biased AG (AG_b), defined as $AG_b = BA_b - CA$, is the difference between a subject's CA and her/his bias-corrected BA. Let CA be an $N \times 1$ vector containing the CAs of all N subjects, and similarly for BA. The Euclidean norms of these vectors are $||CA||$ and $||BA||$, respectively. Let $\rho(BA, CA)$ be the correlation coefficient between CA and BA, as computed using the *corr* function in MATLAB (MathWorks, Natick, MA). Then, for each subject i, $BA_{c,i}$ can be computed (30) as

$$BA_{c,i} = CA_i + AG_{b,i}\frac{||CA||}{\rho(BA, CA)||BA||}$$

Once calculated, BA_c is used to compute the mean absolute error (MAE) of the bias-corrected BA estimate BA_c; the MAE quantifies each brain feature's ability to estimate BA. Using MAE, we quantified the relative ability of each of the four feature types considered here (i.e., regional total volume, total surface area, mean cortical thickness, and mean curvature) to estimate BA.

Calculation of BA after mTBI. For each feature type and anatomic structure, the linear model whose regression coefficients were calculated for HCs is used to estimate BAs for each mTBI participant. In other words, for each mTBI participant, we estimated BA using the HC model as a reference for typical aging. For each subject, we then calculated AG as previously described. For each feature type and structure, the mean AG over subjects provides a mean BA difference between mTBI and HC participants that conveys the amount of excessive aging due to mTBI alone.

Cognitive scores predicted by AGs. For mTBI participants, j = 6 separate linear regressions predicted each cognitive score c_j , where $j \in [1, \ldots, 6]$ is one of the six cognitive scores (EVMI, EVMD, WMS, IR, VF, or PS) being predicted by the regression in question. To yield standardized regression coefficients β, all regression variables (i.e., cognitive scores, CA, and all AGs) were converted to *z*-scores before being used as regressors. In the *omnibus* model, c_j was predicted using CA and the AGs of all M regional volumes, i.e., $c_j = \alpha_j + \beta_j \mathrm{CA} + \beta_{1j} AG_1 + \cdots + \beta_{Mj} AG_M$, where M = 83 is the number of brain regions. To study whether AGs, when considered all together, had significant utility in predicting cognitive scores above and beyond CA, j = 6 linear regressions were also performed to predict c_j using a *reduced* model that included only CA as independent predictor, according to the equation $c_j = \alpha_j + \beta_j CA$. For each cognitive score, the R^2 of the reduced (CA only) model was subtracted from the R^2 of the omnibus (CA *and* AG) model, to quantify the extent to which the omnibus model explained more variance than the reduced model.

Results

Because our models predict CA using *regional* rather than *global* (whole brain) measures, the MAEs reported below reflect each model's average error across *both* regions *and* participants, rather than *only* across participants. The latter is typically the case for most other "whole brain" models that estimate *global*—rather than *regional*—BAs. Linear models regressing CA against each region's mean curvature, surface area, or mean cortical thickness had bias-corrected MAEs that reflected either extreme regression to the mean or minimal, if any, correlation with CA given the mean age and

standard deviation of the sample (surface area MAE across regions = 82 y, σ across regions = 57 y; cortical thickness MAE across regions = 25 y, σ across regions = 2 y; curvature MAE across regions = 16.8 y, σ across regions = 0 y; volume MAE across regions = 17 y, σ across regions = 2 y). In other words, for the average region, the model predicting CA using that region's volume had an MAE of 17 y. These results suggest that volume was considerably more informative than the other three types of anatomic measures. For this reason, most of our results report on volume relative to its dependence on age and use volume for the estimation of regional BAs.

3.1 Regional volumes' dependence on age in HCs. **eTable 1** lists sex-adjusted linear regression coefficients describing HCs' regional volume dependence on age. Negative values of the t test statistic indicate that the dependence of regional volume on CA is steeper in mTBI participants compared to HCs, and vice versa if t is positive. Here and throughout this section, all p-values have been corrected for multiple comparisons. The regions whose *sex-adjusted* regression coefficients are most significantly different from zero pertain (**Figure 1A**), in decreasing order of magnitude, to the nucleus accumbens (β_{HC} ± SE (β_{HC}) = -0.187%/y ± 0.017%/y, t_{3416} = -11.06, p = 5.00×10^{-26}, power > 99%), amygdala (β_{HC} ± SE(β_{HC}) = -0.100%/y ± 0.011%/y, t_{3416} = -9.32, p = 8.35×10^{-19}, power > 99%), lateral orbital sulcus (β_{HC}± SE(β_{HC}) = -0.096%/y ± 0.018%/y, t_{3416} = -5.39, p = 1.96×10^{-7}, power > 99%), posterior transverse collateral sulcus (β_{HC} ± SE(β_{HC}) = -0.091%/y ± 0.017%/y, t_{3416} = -5.20, p = 4.88×10^{-7}, power > 99%), and the collateral and lingual sulcus (β_{HC} ± SE(β_{HC}) = -0.091%/y ± 0.011%/y, t_{3416} = -7.91, p = 3.91×10^{-15}, power > 99%). All regions' significant β_{HC} values are plotted on cortical and subcortical surfaces in **Figure 2**. HCs exhibited no significant sex differences in regression coefficients (all p > 0.05, corrected).

Regional volumes' dependence on age in mTBI. In mTBI participants, as listed in **eTable 2** and plotted in **Figure 1B**, the strongest dependences of regional volume on age were observed in the nucleus accumbens (β_{TBI} ± SE(β_{TBI}) = -0.578%/y ± 0.072%/y; t_{111} = -7.98, p = 1.19×10^{-10}, power > 99%), the middle temporal gyrus (β_{TBI} ± SE(β_{TBI}) = 0.451%/y ± 0.086%/y; t_{111} = -5.26, p = 1.16×10^{-5}, power >

99%), the posterior transverse collateral sulcus (β_{TBI} ± SE(β_{TBI}) = 0.386%/y ± 0.089%/y; t_{111} = -4.31, p = 1.64×10^{-4}, power > 99%), inferior temporal sulcus (β_{TBI} ± SE(β_{TBI}) = 0.368%/y ± 0.073 %/y; t_{111} = -5.07, p = 2.20×10^{-5}, power > 99%), and the thalamus (β_{TBI} ± SE(β_{TBI}) = 0.367%/y ± 0.053%/y; t_{111} = -6.90, p = 1.42×10^{-8}, power > 99%). All regions' significant β_{TBI} values are plotted on cortical and subcortical surfaces in **Figure 3**. mTBI participants exhibited no significant sex differences in regression coefficients (p > 0.05, corrected).

Group comparison of regression coefficients. The regression coefficients of 38 (i.e., 46%) structures differ significantly across HC and mTBI groups (**eTable 3**, **Figure 1C**). These structures are in all lobes of both hemispheres. In mTBI participants, all but nine brain structures exhibit sex-adjusted linear regression coefficients whose magnitudes are at least twice as large as those observed in HCs. When comparing mTBI participants to HCs, the structures with the most significant differences in sex-adjusted β coefficients are (A) the thalamus β_{HC} ± SE(β_{HC}) = -0.077%/y ± 0.009%/y; β_{TBI} ± SE(β_{TBI}) = -0.367%/y ± 0.053%/y, z = -5.37, p = 6.40×10^{-6}, power > 99%; β_{TBI}/β_{HC} = 4.8, (B) the nucleus accumbens (β_{HC} ± SE(β_{HC}) = -0.187%/y ± 0.017%/y; β_{TBI} ± SE(β_{TBI}) = -0.578%/y ± 0.072%/y, z = -5.26, p = 5.82×10^{-6}, power > 99%; β_{TBI}/β_{HC} = 3.09, (C) the cerebellum (β_{HC} ± SE(β_{HC}) = -0.043%/y ± 0.009%/y; β_{TBI} ± SE(β_{TBI}) = -0.301%/y ± 0.055%/y, z = -4.60, p = 1.19×10^{-4}, power > 99%; β_{TBI}/β_{HC} = 7.0, (D) the middle temporal gyrus (β_{HC} ± SE(β_{HC}) = -0.063%/y ± 0.010%/y and β_{TBI} ± SE(β_{TBI}) = -0.451%/y ± 0.086%/y, z = -4.50, p = 1.39×10^{-4}, power > 99%, β_{TBI}/β_{HC} = 7.2), and (E) the anterior cingulate gyrus (β_{HC} ± SE(β_{HC}) = -0.54%/y ± 0.009%/y; β_{TBI} ± SE(β_{TBI}) = -0.278%/y ± 0.053%/y, z = -4.19, p = 4.67×10^{-4}, power > 99%; β_{TBI}/β_{HC} = 5.2).

BA estimates. Aside from modeling the dependence of regional volumes on CA, we used regional volumes to estimate the BAs of HC subjects. As already noted, the bias-corrected linear models describing HC subjects' regional volume trajectories with age can estimate CA based on regional volumes with a MAE of 17 y (σ = 2 y) across all regions.

In mTBI participants, the linear models generated for the HC participants were used to compute regional BAs. Across all cerebral cortical regions, the average AG over structures mapped in mTBI participants was 9.2 years, with a standard deviation of 1.1 years. In other words, in mTBI participants assessed six months after injury, the typical (average) brain region was 9.2 years older, biologically, than in HC participants with the same CA. The structures that exhibited the largest average AGs include the posterior-dorsal cingulate gyrus (11.6 y), middle frontal gyrus (11.3 y), middle temporal gyrus (11.2 y), orbital sulci (11.0 y), and superior frontal gyrus (10.9 y). Conversely, the structures with the lowest AGs include the nucleus accumbens (4.0 y), thalamus (5.4 y), amygdala (6.0 y), putamen (6.5 y), and the hippocampus (7.2 y). Thus, in mTBI participants, the region with the largest average amount of mTBI-related aging is the posterior dorsal aspect of the cingulate gyrus. In the average mTBI participant, this region is 11.6 y older than in the typical HC participant of the same CA. Similarly, the region with the smallest average amount of mTBI-related aging is the nucleus accumbens. In the average mTBI participant, this region is only 4.0 y older than in the typical HC participant of the same CA.

Prediction of cognitive scores. Results for the linear regressions predicting cognitive scores using omnibus (CA and AGs) and reduced (CA only) models are reported in eTable 4. Compared to the CA-only model, inclusion of regional AGs in the omnibus model explained significantly more variance for EVMI and WMS (20.74% and 12.77% more variance, respectively, in the omnibus model compared to the reduced model). The omnibus and reduced models explained similar amounts of variance for IR, VF, and PS (1.60%, 0.49%, and -0.80% additional variance explained by the omnibus model compared to the reduced model). For EVMD, the omnibus model explained significantly less variance (-9.96%) compared to the reduced model.

The brain regions with the largest standardized β magnitudes contributed the most to explaining cognitive aging above and beyond CA (eTable 5). For EVMI, these were the precentral gyrus, calcarine sulcus, and lateral superior temporal gyrus. For EVMD, they were the inferior frontal gyrus,

calcarine sulcus, collateral and lingual sulci, middle frontal gyrus, and precentral sulcus. For WMS, they were the middle frontal gyrus, inferior frontal gyrus, lateral superior temporal gyrus, orbital gyrus, postcentral gyrus, superior temporal gyrus, orbital sulcus, subparietal sulcus, inferior occipital gyrus/sulcus, parieto-occipital sulcus, and parahippocampal gyrus.

Discussion

Interpretation of findings. The most significant group differences in how regional volume depends on age were observed in the thalamus, nucleus accumbens, cerebellum, middle temporal gyrus, and in the anterior cingulate gyrus and sulcus (**eTable 3**). Our study reveals the relative vulnerability of brain structures to mTBI-related aging above and beyond any aging due to typical senescence like that observed in HC participants. Our modelling highlights the posterior dorsal aspect of the cingulate gyrus as being most susceptible to mTBI-related aging effects, whereas the nucleus accumbens is least susceptible. Thus, the nucleus accumbens may be more resilient to mTBI-related aging compared to other brain regions. This structure may also better reflect typical aging processes compared to other regions, as we reported elsewhere for HC participants (33). Prior literature has highlighted the importance of subcortical structures like the nucleus accumbens in a variety of cognitive tasks, including task switching behavior, financial risk taking, cognitive-motor dual tasks, and memory-tasks, all of which are often affected by mTBI (34). The prominence of mTBI-related effects on the subcortex is also highlighted by findings of subcortical neurodegeneration during the chronic stage of mTBI (35).

The subcortical structure with the largest TBI-related effect on regional aging, as reflected by the group difference in regression coefficients β_{TBI} - β_{HC} (z = -5.4) is the thalamus. Aside from mTBI, conditions such as mild cognitive impairment, AD, multiple sclerosis, and Parkinson's disease also demonstrate thalamic atrophy (36). Findings of thalamic vulnerability to disease processes is interesting in the context of symptomatic associations between thalamic volume and increased sensory sensitivities, sleep disruption, and cognition, as found both in mTBI subjects (37) and in

neurodegenerative disease (38). Longitudinal studies indicate that thalamic atrophy is frequently caused by mTBI and is associated with functional outcome (39). Our finding of significantly greater thalamic atrophy in mTBI participants compared to HCs confirms that this region is susceptible to injury, disease, and aging. Our results also highlight the importance of future studies to explain this vulnerability mechanistically in view of formulating strategies to reduce it. This is of note given the evidence that TBI exacerbates neurodegenerative processes leading to higher risk for AD (40).

Our findings also identify the nucleus accumbens as particularly sensitive to typical aging and to mTBI-related effects on aging. Thus, in both HCs and mTBI participants, this structure exhibits the strongest dependence of volume on age. Relative to HCs, this nucleus also has the largest mTBI-related increase in the rate of volume decrease with age. In healthy adults, the nucleus accumbens has been described as providing an interface between the limbic and motor systems as well as being involved in motivation and reward behavior (41). Furthermore, the nucleus accumbens is implicated in various neurodegenerative diseases including schizophrenia, Parkinson's disease, AD, Huntington's disease (2,42), among other conditions. Because TBI often involves deficits of cognitive control and motor function, future studies should examine the relationship between the BA of the nucleus accumbens and each of these functional domains.

In HCs, the structure with the second strongest dependence of volume on age is the amygdala. This structure frequently atrophies in tandem with the hippocampus, the severity of both phenomena being highly correlated with age-related changes in cognitive performance (43). Age-related atrophy of the amygdala is prominent in AD, where it parallels disease stages and severity of clinical symptoms (44). There, atrophy of the amygdala is also associated prominently with decline in motor behavior (45) and with clinical ratings of cognition such as the Mini Mental State Examination and the Clinical Dementia Rating Sum of Boxes (44).

The middle temporal gyrus is one cortical structure with both strong dependence of volume on age *and* with large mTBI effect on this dependence (**Figure 4, eTable 3**). Previous studies have

found that it is vulnerable to cerebral microbleeds and associated with increased depressive symptoms after mTBI (46). We also found that atrophy (regional volume decrease) of this gyrus predicted lower WMS scores to a greater extent than CA alone, in accordance with previous studies that noted working memory reliance on medial temporal lobe structures (e.g., 47,48). The middle temporal gyrus has been associated with modified functional activity and organization in subjects with mild cognitive impairment and AD (49). This region is further associated with cortical thinning in patients with cognitive impairment or vascular white matter lesions (50). Functional dysfunction implicating the middle temporal gyrus has been associated with reports of depression severity and delayed memory in patients with mild cognitive impairment (51). The volume of the right middle temporal gyrus, a structure equally implicated in affect regulation, has also been positively associated with social anxiety (52). Additionally, increased atrophy of the middle temporal gyrus occurs in patients with mild cognitive impairment who later convert to AD (53), as well as in patients with type 2 diabetes mellitus (54). These findings may reflect incident pre-traumatic morbidities that synergize with mTBI to increase the risk of further neurodegeneration.

One longitudinal study reports that brain atrophy occurs at an average rate of ~4.16%/y after mTBI across all brain regions, compared to 1.49%/y in HCs (10). Our group comparison indicates that, at the macroscale, mTBI participants exhibit a decrease in most regional volumes with age that is at least twice faster than that of HCs. These differences, most of which are significant, pertain to gyri and sulci in the frontal and temporal lobes (**Figure 4**). This may be because most mTBIs are fronto-temporal (55), such that our findings could reflect how primary injuries lead to cortical atrophy in these areas. Aside from cortical atrophy due to neuron loss, our findings may also mirror loss of connectivity due to traumatic axonal injury or to breakdown of the blood-brain barrier, as reflected in the presence or predominance of cerebral microbleeds in frontal and temporal regions (56).

Our findings on mTBI participants' regional BAs may reflect deviations from normality in age-related neuroanatomy trajectories. Amongst nearly all structures examined in mTBI participants, regional volume yielded positive AGs (reflective of older BA). Typically, cortical structures' BAs had little intrasubject variance, which may reflect *global* acceleration of brain aging after mTBI. Notably, however, cortical structures exhibited older BAs, on average, than subcortical regions. Our results on regional brain aging provide insights on the differential rates of post-traumatic cortical aging relative to HCs. Because our study examines the relative aging rates of brain regions using univariate models, our results should not be interpreted as attempting to estimate the overall (global) age of the brain. The fact that we use univariate regression models to predict regional BA may explain why our average MAEs, being computed across brain regions for regional BAs, are larger than those computed by other studies for the *entire* brain using more than one measure. For example, when computed from volume, the MAE of regional BA is 17 y, which considerably more than the typical MAE of ~5 y or less computed by many BA estimators (57). This suggests only that, for the average brain region, the univariate setting used here to calculate *regional* BAs is inadequate for estimating the *global* BA of the *entire* brain. In other words, the volume of the *typical* brain region does not predict CA nearly as well as the weighted sum of *all* regional brain volumes. This is to be expected of most univariate models, which are relatively ill-equipped to explain as much variance as a multivariate model with far more explanatory variables. Furthermore, our MAEs computed *across regions* merely reflect *regional* variability in brain aging and should *not* be compared against the (often much smaller) MAEs of models that quantify the variability of *global* brain aging *across subjects*. Indeed, it would be unexpected to encounter such low MAEs when using a univariate model to capture because such a model cannot explain as much variance as a multivariate (whole-brain) BA estimation model like the one that we reported elsewhere (33) and that yielded an MAE of 6.6 years when computed across all mTBI participants studied here.

Some regional brain volumes were found to reflect significantly more cognitive score variability than predicted by CA and were significant at an uncorrected level ($p < 0.05$, see eTable 5).

When predicting EVMI and WMS scores, the inclusion of AGs contributed significantly, over and above CA, to explaining model variance. We did not expect that any single region's volume could explain any of our cognitive measures partly because cognitive aging is mediated by many biological processes (e.g., reductions of dendritic complexity leading to subtle morphometry changes across more than one parcel) that are not captured well by macroscale imaging measures like ours (58,59). Furthermore, cognitive measures often rely on processes that recruit many discontiguous regions, such that a single region's macroscale atrophy rarely reflects the complex brain processes that explain cognitive scores.

Limitations and comparison to other studies. Although our reported findings are significant and rely on well-powered tests, the cross-sectional nature of our data is a limitation because our computed rates of volume alterations with age cannot be equated to atrophy rates. Nevertheless, despite modest follow-up periods, sample sizes, and aggregation across TBI severities, longitudinal studies corroborate our findings on the thalamus (60), nucleus accumbens (61), and middle frontal gyrus (62). Conversely, whereas our sample size is larger than those of similar studies, our study is limited by its cross-sectional nature. Thus, to establish how mTBI causes the brain to atrophy as a function of age at injury, future research should investigate post-traumatic regional atrophy longitudinally using approaches that can resolve biological mechanisms.

One limitation of our study is the fact that it aggregates data from several sources, such that the variance due to differences across cohorts must be considered. Because HC and mTBI participants had not been scanned as part of the same study, we aggregated HC data from several repositories to provide comparisons that reflect inter-scanner heterogeneity (e.g., differences in scanning parameters). Although the statistical effects of cohort, sex, and FS version were regressed out, confounds related to scanner type, acquisition site, sequence parameters, and to other factors were not accounted for here and may, in fact, be difficult or even impossible to capture adequately using linear regression. The limitations of standard statistical models extend to our calculated

associations between age and brain features. Here, extending our analysis to higher-order models was not attempted due to the dangers of overfitting, to the difficulty of interpreting higher-order models, and to their potentially incremental insights of such models despite their complexity. Nevertheless, future studies should investigate nonlinear relationships between regional volumes and age at injury to further describe the effects of TBI on the aging brain.

Finally, rather than focusing on laterality effects, we averaged regional volumes across hemispheres before implementing linear regression of volume on age. Our motivation for this was the fact that spatial TBI patterns are often neuroanatomically asymmetric, and this confound cannot be accounted for adequately without averaging across hemispheres unless detailed information on spatial injury profiles is available. Nevertheless, laterality effects warrant investigation, as the interaction between TBI location and the functional correlates of laterality (e.g., handedness) can provide insight into the dependence of regional volumes on age, both in typical aging and after TBI.

Conclusion

The results of our study provide a uniquely granular approach to the volumetric neuroanatomical changes in victims of mTBI relative to an HC cohort. Strikingly, in an adult cohort that spans a wide age range, we observe significantly greater decreases in regional volumes with age in mTBI subjects compared to HCs. Furthermore, when used to estimate age using linear models, regional volumes of the brain reveal significantly older BA in mTBI participants than in HCs of the same age and sex. In concert, these results offer a valuable foundation for future investigations on how mTBI affects brain BA.

Funding

This work was supported by the National Institutes of Health grant R01 NS 100973 to A.I., by the US Department of Defense contract W81XWH-18-1-0413 to A.I., by a Hanson-Thorell Family Research Scholarship, and by the James J. and Sue Femino Foundation. Data were provided, in part, by the Human Connectome Project, WU-Minn Consortium (Principal Investigators: David Van Essen and Kamil Ugurbil; 1U54 MH 091657) funded by the 16 NIH Institutes and Centers that support the NIH Blueprint for Neuroscience Research, and by the McDonnell Center for Systems Neuroscience at Washington University. Data collection and sharing for this project was funded by the Alzheimer's Disease Neuroimaging Initiative (ADNI, National Institutes of Health Grant U01 AG024904) and DoD ADNI (Department of Defense award number W81XWH-12-2-0012). ADNI is funded by the National Institute on Aging, the National Institute of Biomedical Imaging and Bioengineering, and through generous contributions from the following: AbbVie, Alzheimer's Association; Alzheimer's Drug Discovery Foundation; Araclon Biotech; BioClinica, Inc.; Biogen; Bristol-Myers Squibb Company; CereSpir, Inc.; Cogstate; Eisai Inc.; Elan Pharmaceuticals, Inc.; Eli Lilly and Company; EuroImmun; F. Hoffmann-La Roche Ltd and its affiliated company Genentech, Inc.; Fujirebio; GE Healthcare; IXICO Ltd.; Janssen Alzheimer Immunotherapy Research & Development, LLC.; Johnson & Johnson Pharmaceutical Research & Development LLC.; Lumosity; Lundbeck; Merck & Co., Inc.; Meso Scale Diagnostics, LLC.; NeuroRx Research; Neurotrack Technologies; Novartis Pharmaceuticals Corporation; Pfizer Inc.; Piramal Imaging; Servier; Takeda Pharmaceutical Company; and Transition Therapeutics. The Canadian Institutes of Health Research is providing funds to support ADNI clinical sites in Canada. Private sector contributions are facilitated by the Foundation for the National Institutes of Health (www.fnih.org). The grantee organization is the Northern California Institute for Research and Education, and the study is coordinated by the Alzheimer's Therapeutic Research Institute at the University of Southern California. ADNI data are disseminated by the Laboratory for Neuro Imaging at the University of Southern California.

Data sourced from TRACK-TBI were acquired with funding from the U.S. National Institutes of Health, National Institute of Neurologic Disorders and Stroke (TRACK-TBI NINDS Grant U01 NS1365885), and from public and private partners. The opinions or assertions contained here are the private views of the authors and are not to be construed as official or as reflecting the views of any sponsor.

Acknowledgements

A.F.S. led study design, software development, data analysis, manuscript redaction, and figure preparation and contributed to study conceptualization and data curation. R.J.M. contributed to data curation, study design, software development, and manuscript redaction. P.I. contributed to data analysis, manuscript editing and reviewing. R.V.V. contributed to manuscript redaction and figure preparation. A.A. contributed to data curation, study design, and data analysis. A.I. led study conceptualization, funding acquisition, and manuscript reviewing, and contributed to all other project aspects. We thank Chur Tam and Dylan Overby for assistance with figure preparation and literature searches.

Conflict of Interest

The authors declare no conflict of interest.

References

1. Raz N, Rodrigue KM. Differential aging of the brain: Patterns, cognitive correlates and modifiers. *Neuroscience & Biobehavioral Reviews.* 2006;30(6):730-748.
2. Cole JH, Ritchie SJ, Bastin ME, et al. Brain age predicts mortality. *Molecular Psychiatry.* 2018;23(5):1385-1392.
3. Baecker L, Dafflon J, Da Costa PF, et al. Brain age prediction: A comparison between machine learning models using region- and voxel- based morphometric data. *Human Brain Mapping.* 2021;42(8):2332-2346.
4. Cheng J, Liu Z, Guan H, et al. Brain age estimation from MRI using cascade networks with ranking loss. *IEEE Transactions on Medical Imaging.* 2021;40(12):3400-3412.
5. Tseng W-YI, Hsu Y-C, Kao T-W. Brain age difference at baseline predicts clinical dementia rating change in approximately two years. *Journal of Alzheimer's Disease.* 2022;86(2):613-627.
6. Grueso S, Viejo-Sobera R. Machine learning methods for predicting progression from mild cognitive impairment to Alzheimer's disease dementia: a systematic review. *Alzheimer's Research & Therapy.* 2021;13(1):1-29.
7. Beheshti I, Ganaie M, Paliwal V, Rastogi A, Razzak I, Tanveer M. Predicting brain age using machine learning algorithms: A comprehensive evaluation. *IEEE Journal of Biomedical and Health Informatics.* 2021;26(4):1432-1440.
8. Dennis EL, Taylor BA, Newsome MR, et al. Advanced brain age in deployment-related traumatic brain injury: A LIMBIC-CENC neuroimaging study. *Brain Injury.* 2022;36(5):662-672.

9. Abdul-Muneer P, Chandra N, Haorah J. Interactions of oxidative stress and neurovascular inflammation in the pathogenesis of traumatic brain injury. *Molecular Neurobiology.* 2015;51(3):966-979.

10. MacKenzie JD, Siddiqi F, Babb JS, et al. Brain atrophy in mild or moderate traumatic brain injury: A longitudinal quantitative analysis. *American Journal of Neuroradiology.* 2002;23(9):1509-1515.

11. Spitz G, Bigler ED, Abildskov T, Maller JJ, O'Sullivan R, Ponsford JL. Regional cortical volume and cognitive functioning following traumatic brain injury. *Brain and Cognition.* 2013;83(1):34-44.

12. Driscoll I, Davatzikos C, An Y, et al. Longitudinal pattern of regional brain volume change differentiates normal aging from MCI. *Neurology.* 2009;72(22):1906-1913.

13. Shao M, Cao J, Bai L, et al. Preliminary evidence of sex differences in cortical thickness following acute mild traumatic brain injury. *Frontiers in Neurology.* 2018;9:878.

14. Teasdale G, Jennett B. Assessment of coma and impaired consciousness: A practical scale. *The Lancet.* 1974;304(7872):81-84.

15. Rostowsky KA, Irimia A. Acute cognitive impairment after traumatic brain injury predicts the occurrence of brain atrophy patterns similar to those observed in Alzheimer's disease. *GeroScience.* 2021;43(4):2015-2039.

16. Hutchinson EB, Schwerin SC, Radomski KL, et al. Detection and distinction of mild brain injury effects in a ferret model using diffusion tensor MRI (DTI) and DTI-driven tensor-based morphometry (D-TBM). *Frontiers in Neuroscience.* 2018;12:573.

17. Tun PA, Lachman ME. Telephone assessment of cognitive function in adulthood: The Brief Test of Adult Cognition by Telephone. *Age and Ageing.* 2006;35(6):629-632.

18. Lachman ME, Agrigoroaei S, Tun PA, Weaver SL. Monitoring cognitive functioning: Psychometric properties of the brief test of adult cognition by telephone. *Assessment.* 2014;21(4):404-417.

19. Glasser MF, Smith SM, Marcus DS, et al. The human connectome project's neuroimaging approach. *Nature Neuroscience.* 2016;19(9):1175-1187.

20. Littlejohns TJ, Holliday J, Gibson LM, et al. The UK Biobank imaging enhancement of 100,000 participants: Rationale, data collection, management and future directions. *Nature Communications.* 2020;11(1):1-12.

21. Petersen RC, Aisen P, Beckett LA, et al. Alzheimer's disease neuroimaging initiative (ADNI): Clinical characterization. *Neurology.* 2010;74(3):201-209.

22. Yue JK, Vassar MJ, Lingsma HF, et al. Transforming research and clinical knowledge in traumatic brain injury pilot: Multicenter implementation of the common data elements for traumatic brain injury. *Journal of Neurotrauma.* 2013;30(22):1831-1844.

23. Dale AM, Fischl B, Sereno MI. Cortical surface-based analysis: I. Segmentation and surface reconstruction. *NeuroImage.* 1999;9(2):179-194.

24. Fischl B, Sereno MI, Dale AM. Cortical surface-based analysis: II: Inflation, flattening, and a surface-based coordinate system. *NeuroImage.* 1999;9(2):195-207.

25. Irimia A, Chambers MC, Torgerson CM, Van Horn JD. Circular representation of human cortical networks for subject and population-level connectomic visualization. *NeuroImage.* 2012;60(2):1340-1351.

26. Lee H, Wintermark M, Gean AD, Ghajar J, Manley GT, Mukherjee P. Focal lesions in acute mild traumatic brain injury and neurocognitive outcome: CT versus 3T MRI. *Journal of Neurotrauma.* 2008;25(9):1049-1056.

27. Clogg CC, Petkova E, Haritou A. Statistical methods for comparing regression coefficients between models. *American Journal of Sociology.* 1995;100(5):1261-1293.

28. Benjamini Y, Hochberg Y. Controlling the false discovery rate: A practical and powerful approach to multiple testing. *Journal of the Royal Statistical Society: Series B (Methodological).* 1995;57(1):289-300.

29. Irimia A, Torgerson CM, Goh S-YM, Van Horn JD. Statistical estimation of physiological brain age as a descriptor of senescence rate during adulthood. *Brain Imaging and Behavior.* 2015;9(4):678-689.

30. Treder MS, Shock JP, Stein DJ, Du Plessis S, Seedat S, Tsvetanov KA. Correlation constraints for regression models: Controlling bias in brain age prediction. *Frontiers in Psychiatry.* 2021;12:615754.

31. Beheshti I, Nugent S, Potvin O, Duchesne S. Bias-adjustment in neuroimaging-based brain age frameworks: A robust scheme. *NeuroImage: Clinical.* 2019;24:102063.

32. Cole JH, Leech R, Sharp DJ, Initiative AsDN. Prediction of brain age suggests accelerated atrophy after traumatic brain injury. *Annals of Neurology.* 2015;77(4):571-581.

33. Massett RJ, Maher AS, Imms PE, et al. Regional neuroanatomic effects on brain age inferred using magnetic resonance imaging and ridge regression. *The Journals of Gerontology: Series A.* 2022.

34. de Freitas Cardoso MG, Faleiro RM, De Paula JJ, et al. Cognitive impairment following acute mild traumatic brain injury. *Frontiers in Neurology.* 2019;10:198.

35. Sandry J, Dobryakova E. Global hippocampal and selective thalamic nuclei atrophy differentiate chronic TBI from Non-TBI. *Cortex.* 2021;145:37-56.

36. Štepán-Buksakowska I, Szabó N, Horínek D, et al. Cortical and subcortical atrophy in Alzheimer disease: Parallel atrophy of thalamus and hippocampus. *Alzheimer Disease & Associated Disorders.* 2014;28(1):65-72.

37. Sours C, George EO, Zhuo J, Roys S, Gullapalli RP. Hyper-connectivity of the thalamus during early stages following mild traumatic brain injury. *Brain Imaging and Behavior.* 2015;9(3):550-563.

38. Foo H, Mak E, Yong T, et al. Progression of subcortical atrophy in mild Parkinson's disease and its impact on cognition. *European Journal of Neurology.* 2017;24(2):341-348.

39. Lutkenhoff ES, Wright MJ, Shrestha V, et al. The subcortical basis of outcome and cognitive impairment in TBI: A longitudinal cohort study. *Neurology.* 2020;95(17):e2398-e2408.

40. Imms P, Chui HC, Irimia A. Alzheimer's disease after mild traumatic brain injury. *Aging.* 2022;14(13):5292.

41. Goto Y, Grace AA. Dopaminergic modulation of limbic and cortical drive of nucleus accumbens in goal-directed behavior. *Nature Neuroscience.* 2005;8(6):805-812.

42. Bayassi-Jakowicka M, Lietzau G, Czuba E, Patrone C, Kowiański P. More than addiction: The nucleus accumbens contribution to development of mental disorders and neurodegenerative diseases. *International Journal of Molecular Sciences.* 2022;23(5):2618.

43. Heun R, Mazanek M, Atzor K-R, et al. Amygdala-hippocampal atrophy and memory performance in dementia of Alzheimer type. *Dementia and Geriatric Cognitive Disorders.* 1997;8(6):329-336.

44. Poulin SP, Dautoff R, Morris JC, Barrett LF, Dickerson BC, Initiative AsDN. Amygdala atrophy is prominent in early Alzheimer's disease and relates to symptom severity. *Psychiatry Research: Neuroimaging.* 2011;194(1):7-13.

45. Ahveninen LM, Stout JC, Georgiou-Karistianis N, Lorenzetti V, Glikmann-Johnston Y. Reduced amygdala volumes are related to motor and cognitive signs in Huntington's disease: The IMAGE-HD study. *NeuroImage: Clinical.* 2018;18:881-887.

46. McKee AC, Robinson ME. Military- related traumatic brain injury and neurodegeneration. *Alzheimer's & Dementia.* 2014;10(3 Suppl):S242-S253.

47. Jeneson A, Squire LR. Working memory, long-term memory, and medial temporal lobe function. *Learning & Memory.* 2012;19(1):15-25.

48. Wagner DD, Sziklas V, Garver KE, Jones-Gotman M. Material-specific lateralization of working memory in the medial temporal lobe. *Neuropsychologia.* 2009;47(1):112-122.

49. Zhou B, Liu Y, Zhang Z, et al. Impaired functional connectivity of the thalamus in Alzheimer's disease and mild cognitive impairment: A resting-state fMRI study. *Current Alzheimer Research.* 2013;10(7):754-766.

50. Liu Y, Hu A, Chen L, et al. Association between cortical thickness and distinct vascular cognitive impairment and dementia in patients with white matter lesions. *Experimental Physiology.* 2021;106(7):1612-1620.

51. Dong Q-Y, Li T-R, Jiang X-Y, Wang X-N, Han Y, Jiang J-H. Glucose metabolism in the right middle temporal gyrus could be a potential biomarker for subjective cognitive decline: A study of a Han population. *Alzheimer's Research & Therapy.* 2021;13(1):1-12.

52. Wang S, Zhao Y, Wang X, et al. Emotional intelligence mediates the association between middle temporal gyrus gray matter volume and social anxiety in late adolescence. *European Child & Adolescent Psychiatry.* 2021;30(12):1857-1869.

53. Tseng LH, Chou CY. A longitudinal voxel-based morphometry study of GM atrophy progression. In: *Information Technology and Computer Application Engineering.* CRC Press; 2013:665-670.

54. Li C, Jin R, Liu K, et al. White matter atrophy in type 2 diabetes mellitus patients with mild cognitive impairment. *Frontiers in Neuroscience.* 2021;14:602501.

55. Irimia A, Goh S-YM, Wade AC, Patel K, Vespa PM, Van Horn JD. Traumatic brain injury severity, neuropathophysiology, and clinical outcome: Insights from multimodal neuroimaging. *Frontiers in Neurology.* 2017;8:530.

56. Van der Horn H, de Haan S, Spikman J, de Groot JC, van der Naalt J. Clinical relevance of microhemorrhagic lesions in subacute mild traumatic brain injury. *Brain Imaging and Behavior.* 2018;12(3):912-916.

57. Yin C, Imms P, Cheng M, et al. Anatomically interpretable deep learning of brain age captures domain-specific cognitive impairment. *Proceedings of the National Academy of Sciences.* 2023;120(2):e2214634120.

58. Burke SN, Barnes CA. Neural plasticity in the ageing brain. *Nature Reviews Neuroscience.* 2006;7(1):30-40.

59. Cox SR, Bastin ME, Ritchie SJ, et al. Brain cortical characteristics of lifetime cognitive ageing. *Brain Structure and Function.* 2018;223(1):509-518.

60. Warner MA, Youn TS, Davis T, et al. Regionally selective atrophy after traumatic axonal injury. *Archives of Neurology.* 2010;67(11):1336-1344.

61. Hellstrøm T, Westlye LT, Sigurdardottir S, et al. Longitudinal changes in brain morphology from 4 weeks to 12 months after mild traumatic brain injury:

Associations with cognitive functions and clinical variables. *Brain Injury*. 2017;31(5):674-685.

62. Muller AM, Panenka WJ, Lange RT, Iverson GL, Brubacher JR, Virji- Babul N. Longitudinal changes in brain parenchyma due to mild traumatic brain injury during the first year after injury. *Brain and Behavior*. 2021;11(12):e2410.

Tables

Table 1. Participant demographics. For each cohort, the sample size n and number of females are listed. For age, the range, mean (μ), and standard deviation (σ) of each cohort are listed in years (y).

			age [y]		
HC cohort	n[a]	females	range	μ[b]	σ[c]
ADNI	513	278	56 – 95	75	7
HCP-A	508	294	36 – 80	56	12
HCP-YA	1112	605	22 – 37	29	4
UK Biobank	1285	676	45 – 83	63	10
all	3418	1853	22 – 95	53	19
TBI cohort	113	44	21 – 83	43	17

Note. Cam-CAN=Cambridge Centre for Ageing and Neuroscience, HCP-A=Human Connectome Project Aging, HCP-YA=Human Connectome Project Young Adult.

n[a]=sample size

μ[b]=mean age of sample

σ[c]=standard deviation of age of sample

Figure Captions

Figure 1. Comparison of selected regression coefficients β reflecting age-related rates of regional brain volume change in (A) HCs (β_{HC}), (B) TBI participants (β_{TBI}). (C) The ratio β_{TBI}/β_{HC} conveys the factor whereby regional rates of volume change are higher in mTBI participants compared to the HC reference. The six structures listed in (A), (B) and (C) have the largest magnitudes of β_{HC}, β_{TBI} and β_{TBI}/β_{HC}, respectively. Thus, in (A) and (B), the structures listed have the fastest rates of volume decrease with age in HCs and mTBI participants, respectively. In (C) the structures listed are those whose rate of volume decrease with age are most affected by TBI relative to all other regions.

Figure 2. Regression coefficients β_{HC} obtained from regional volumetric models of healthy control participants plotted as a heatmap on a model cortical surface and subcortical features. Gray color indicates that the test of H_0: $\beta_{HC} = 0$ had statistical power under 80% or a p-value below 0.05 after Benjamini-Hochberg correction for multiple comparisons. Darker red hues indicate a more negative β_{HC}, and therefore a stronger dependence of regional volume on age.

Figure 3. Regression coefficients β_{TBI} obtained from regional volumetric models of mild traumatic brain injury participants plotted as a heatmap on a model cortical surface and subcortical features. Gray color indicates that the test of H_0: $\beta_{TBI} = 0$ had statistical power under 80% or a p-value below 0.05 after Benjamini-Hochberg correction for multiple comparisons. Darker red hues indicate a more negative β_{TBI}, and therefore a stronger dependence of regional volume on age.

Figure 4. The ratio of regression coefficients β_{TBI}/β_{HC}, obtained from regional volumetric models of either mild traumatic brain injury or healthy control participants, plotted as a heatmap on a model

cortical surface and subcortical features. Gray color indicates that the test of $H_0: \frac{(\beta_{TBI}-\beta_{HC})}{\sqrt{SE(\beta_{TBI})+SE(\beta_{HC})}} = 0$ had statistical power under 80% or a p-value below 0.05 after Benjamini-Hochberg correction for multiple comparisons. Darker red hues indicate higher values of the ratio β_{TBI}/β_{HC}, and therefore a more significant change in regression coefficients die to mild traumatic brain injury.

Figure 1

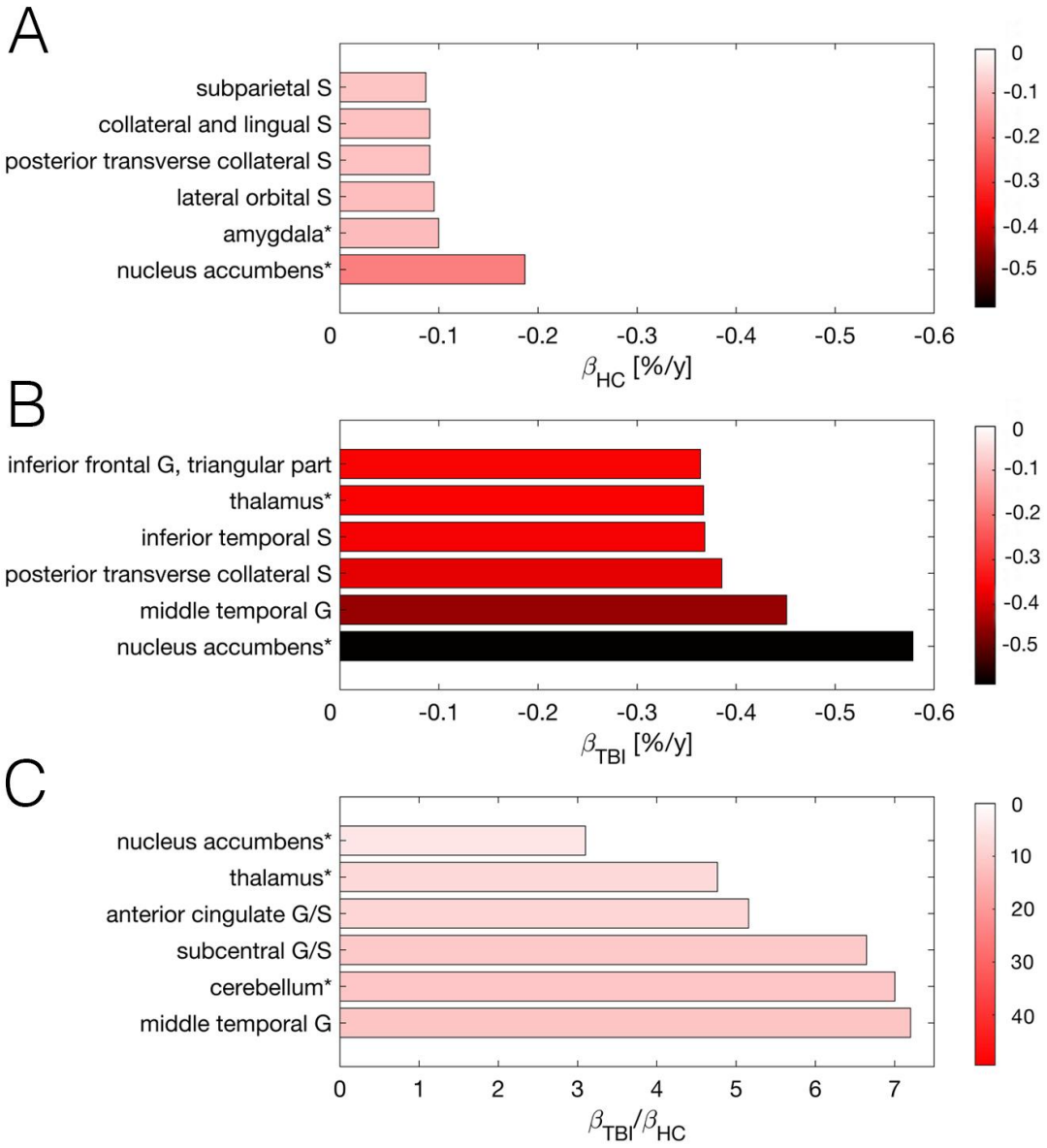

Figure 2

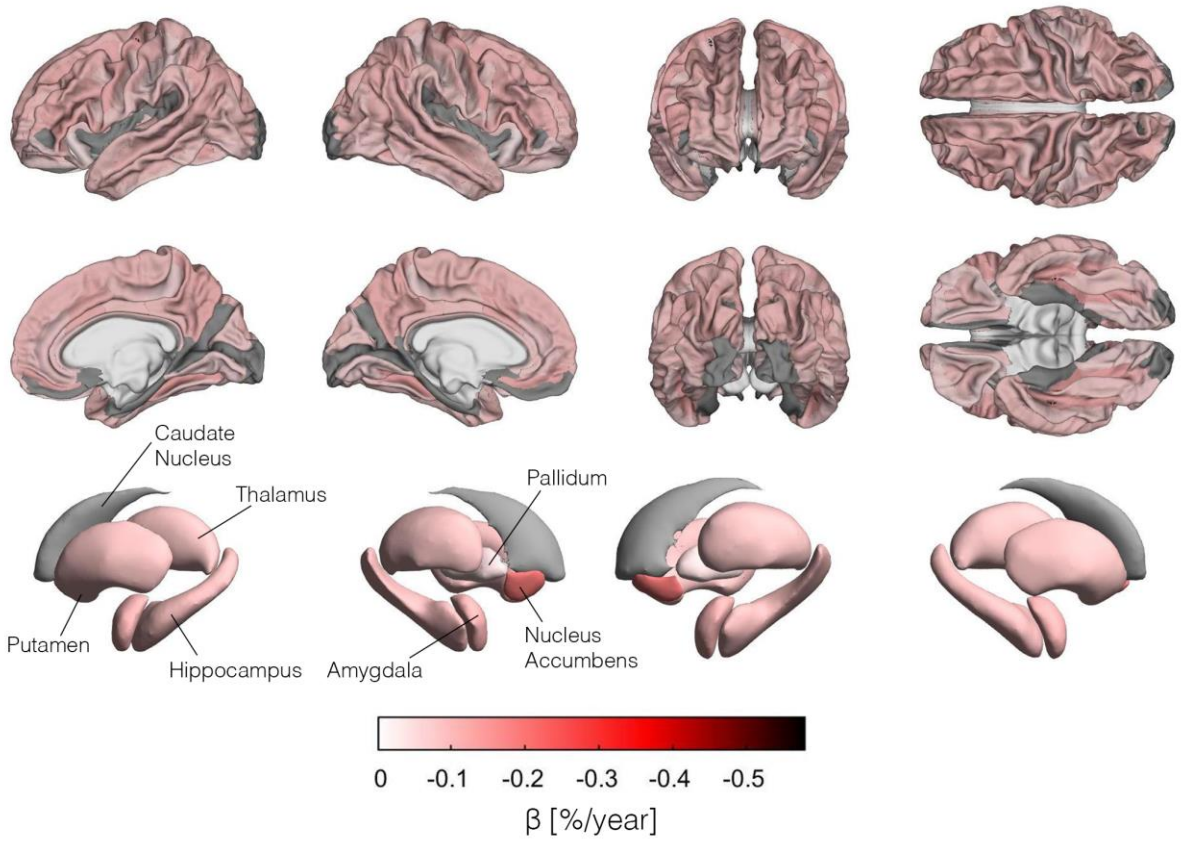

Figure 3

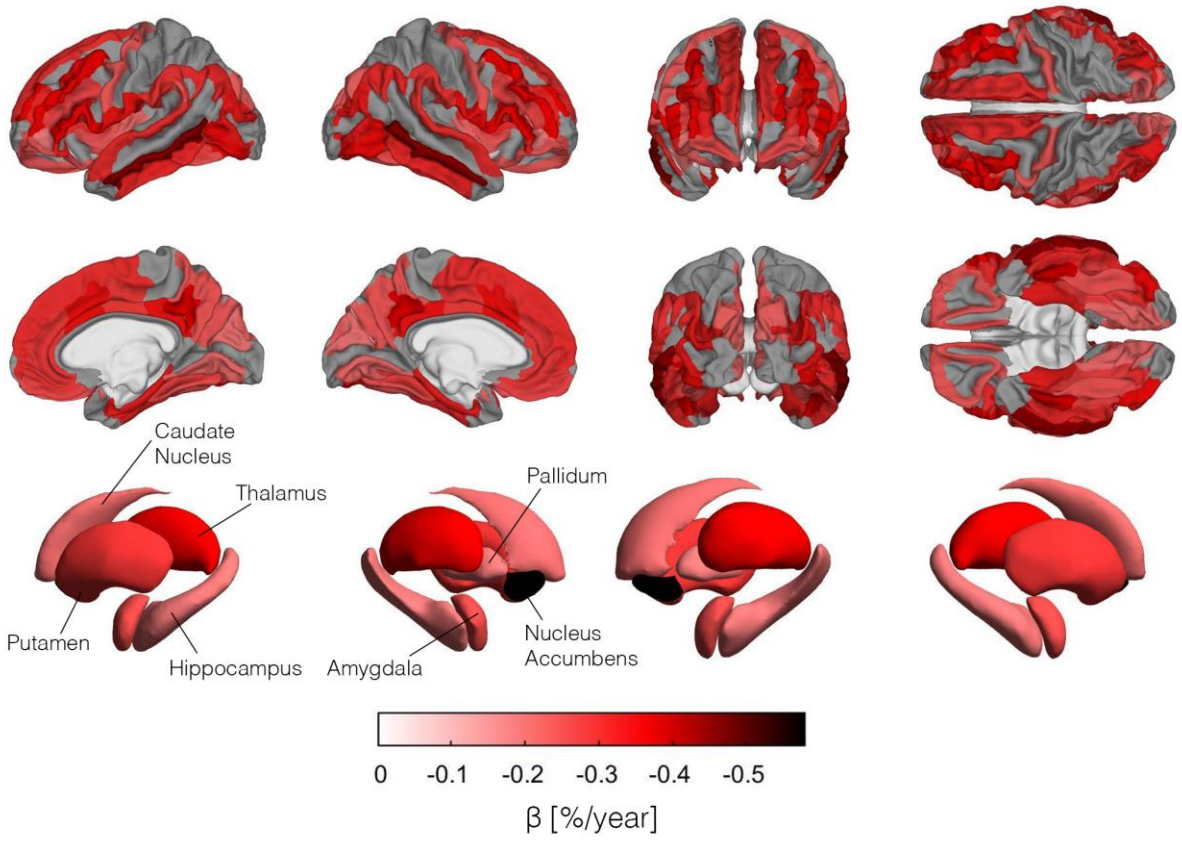

Figure 4